Luminescence depreciation in ScVO4:Bi3+ upon irradiation in the Bi3+-related absorption bands

Philippe Boutinaud, Anthony Barros, Fengwen Kang

Version of Record: https://www.sciencedirect.com/science/article/pii/S0022231322002162
Manuscript_a5cca879fa8fae8dd7ea76b5f58c3128

Luminescence depreciation in $ScVO_4:Bi^{3+}$ upon irradiation in the Bi^{3+}-related absorption bands

Philippe Boutinaud[1]*, Anthony Barros[1], Fengwen Kang,[2,3]

[1] Université Clermont Auvergne, Clermont Auvergne INP, CNRS, ICCF, F-63000 Clermont–Ferrand, France; [2] Laboratory of Advanced Nano Materials and Devices, Ningbo Institute of Materials Technology and Engineering (NIMTE), Chinese Academy of Sciences (CAS), Ningbo, 315201, China; [3] DTU Fotonik, Department of Photonics Engineering, Technical University of Denmark, Anker Engelunds Vej 1, 2800 Kgs, Lyngby, Denmark.

* Corresponding author: philippe.boutinaud@sigma-clermont.fr

Abstract

Luminescence depreciation is evidenced in $ScVO_4:Bi^{3+}$ at room temperature upon LED irradiation at 375 nm. The depreciation amounts 50% of the initial emission intensity after 13 hours under a power density of 4.8 mW/cm^2. The process is accelerated upon warming. These deleterious phenomena are explained by the photo-stimulated oxidization of Bi^{3+} that is favored in $ScVO_4:Bi^{3+}$ by the presence of lattice defects adjacent to Bi^{3+}.

Keywords : Bi^{3+}, $ScVO_4$, Luminescence depreciation

1. Introduction

Orthovanadates $LnVO_4$ (Ln = Sc, Y, Gd, Lu) doped with Bi^{3+} are known for long to glow in the yellow-red spectral range with high efficiency at room temperature [1,2]. In $ScVO_4:Bi^{3+}$, the luminescence appears as a broad band with a maximum at ≈ 635 nm and a Stokes shift of ≈ 12000 cm^{-1}, in correspondence with the lowest excitation energy of ≈ 27700 cm^{-1} (360 nm). [2-5]. The body color of the 1 mol% Bi^{3+}-doped powder is bright yellow, signifying an absorption in the blue region of the spectrum. Yellow color is frequently observed in vanadate lattices, even not intentionally doped. In YVO_4, for instance, the yellow color is ascribed to oxygen vacancies adjacent to V^{4+} ions forming $[V^{4+}]_A$ centers [6]. Exciting in the blue spectral region does not produce luminescence. The lowest fundamental excitation of $ScVO_4$ is reported at ≈ 30300 cm^{-1} (330 nm) in correspondence with the O^{2-} (2p) → V^{5+} (3d) ligand-to-metal charge transfer taking place within the tetrahedral $[VO_4]^{3-}$ units of the host lattice. The associated emission occurs normally at low temperature in the blue region (≈ 483 nm) [2]. Virgin $ScVO_4$ is sometimes reported to glow at room temperature in the blue-green spectral region [3,7]. In this case, the emission is ascribed to tetrahedral tetroxo $(VO_4)^{3-}$ complex groups perturbed by lattice defects [7]. The electron transitions of Bi^{3+} inserted in transition metals oxides such as orthovanadates occur within the levels of isolated Bi^{3+} ions (*i.e.* intra-ionic transitions) or have a metal-to-metal charge transfer (MMCT) character. In the first situation, the electron transition takes place from the $^1S_0$ ground state of the $6s^2$ configuration to the regular $^3P_1$ (A band), $^3P_2$ (B band) and $^1P_1$ states (C band) of $6s^16p^1$ excited configuration. The C band results from spin-allowed transition and is strong but located far in the UV. The B band is forbidden. The A band is only partially allowed by spin-orbit mixing with $^1P_1$ state. The MMCT transitions take place between Bi^{3+} (the electron donor) and the nearest transition metal cation (the metal acceptor), *i. e.* V^{5+} in the present case [8], forming a trapped exciton. The origin of Bi^{3+} emission in the zircon vanadates YVO_4, $GdVO_4$ and $LuVO_4$ has been the subject of extensive investigation in the past and the Bi-V CT (or excitonic) character of this emission is now clearly established [1, 2, 9-15]. Considering the arguments developed in [16], the excitation path of Bi^{3+} involves the A state and is followed by the photoionization of Bi^{3+} that liberates an electron in the conduction band. This electron is bounded by the coulomb field generated by the Bi^{4+} ion that is left behind and forms the Bi-trapped exciton. $ScVO_4:Bi^{3+}$, however, is comparatively less explored and the situation in this compound is still not completely fixed. Referring to [2], the room temperature emission of $ScVO_4:Bi^{3+}$ occurs at 640 nm with a Stokes shift of 1.51 eV. Boulon proposed to ascribe this

emission to $^3P_1 \rightarrow {}^1S_0$ transitions (*i. e.* transition of A character), stating that the red shift of the emission compared to the yellow emission of the other isotrustural vanadates is due to the ionic mismatch between Bi^{3+} and its doping site. The same attribution was confirmed by Kang *et. al* who infered that the red shift of the emission is caused by the presence of oxygen vacancies adjacent to Bi^{3+} ions [3,4]. The energy downshift of the so-formed V_O-pertubed A state (*i. e.* corresponding to a Bi^{3+} ion in seven-fold coordination in $ScVO_4$) was further supported in [7] where the energy of this state (27880 cm^{-1} (≈ 359 nm)) was calculated close to that of the $V^{5+}(3d^0) \rightarrow Bi^{4+}(6s^1) + V^{4+}(3d^1)$ MMCT state (27360 cm^{-1} (365 nm)). In such a situation, emission from both A and CT states is possible with an intensity ratio depending on temperature [8, 17-19]. When occuring, the A emission usually appears in the UV spectral range with a Stokes shift below ≈ 1 eV and a spectral bandwidth below ≈ 0.35 eV [19]. This relaxation path is favored when the A state is distant from the bottom of the lattice conduction band. Despite the energy proximity of CT and V_O-perturbed A states in $ScVO_4:Bi^{3+}$ and in contradiction with previous assignments, it was concluded in [20] that the red emission is more probably of CT character. In the present work, we investigate the luminescence behavior of $ScVO_4:Bi^{3+}$ exposed to photons of 375 nm (26670 cm^{-1}), *i. e.* below the host fundamental excitation but consistent with the long wavelength tail of the Bi^{3+}-related absorption bands. Efficient depreciation of the luminescence is evidenced under these conditions, even at room temperature. The effect is accelerated by raising temperature. Our motivation is to try understanding the origin of this phenomenon that is not usual for zircon orthovanadates doped with Bi^{3+}. In parallel, we show results that reveal the coexistence of Bi-V CT and Vo-pertubed A emissions in $ScVO_4:Bi^{3+}$.

2. Experimental

The $ScVO_4:Bi^{3+}$ (1%) sample was obtained from Professor Mingying Peng and already thoroughly characterized in previous reports [3-5]. We further checked through Rietveld refinements that its zircon structure (ICSD-78073) was maintained in the temperature range 25 – 200 °C with no significant difference of the structural parameters. A home-made "aging box" was used for the evaluation of the long-term behavior of the phosphor upon the action of different stresses (irradiation power, temperature, hygrometry) taken either independently or combined [21]. The setup consists of a collimated power-controlled LED, a copper-based heating element as sample holder allowing working in the temperature range 20 – 250 °C and a computer-controlled fibered monochromator (Ocean Optics model HR4000) preliminary

calibrated using an Ocean Optics lamp (model HL-3P-Cal). In our experiments, a collimated LED chip from Enfis emitting at 375 ± 10 nm was selected. The relative humidity in the aging box was 40 %. The luminescence spectra were automatically recorded every 2 to 30 minutes depending on the total duration of the experiment (typically between 4 and 300 hours). The luminescence intensity was evaluated as the integrated area below the emission band taken in the range 450 – 900 nm, after background correction. A high-pass filter with a cut-off frequency of 450 nm was positioned at the entrance of the fiber to eliminate any trace of stray light. The reflectivity spectra were recorded using a Shimadzu UV 2600 spectrometer equiped with an integrated sphere. The steady state photoluminescence spectra were collected using an association of TRIAX 180 and TRIAX 550 monochromators from Jobin-Yvon Horiba. The excitation source was a 400W xenon lamp. A R928 photomultiplier from Hamamatsu was used as a detector. The spectra were corrected for spectral responses. The time-resolved emission spectra were collected at room temperature upon 375 nm excitation using an Ekspla OPO laser operated at 10 Hz associated with a FLS 980 spectrophotometer from Edinburgh Instruments.

3. Results and discussion

Before going through the experimental data, we depict in Fig. 1 the host-referred energy level scheme of $ScVO_4:Bi^{3+}$ as deduced from Section 1. In this scheme, the bottom of the conduction band matches the host fundamental excitation and the top of the valence band (of prominent O^{2-} ($2p^6$) character) is positioned at energy 0 and constitutes the energy reference. The bottom of the conduction band (of prominent V^{5+} ($3d^0$) character) is located 30300 cm^{-1} above.

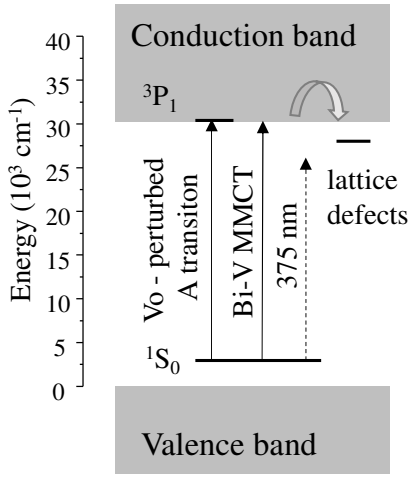

Fig. 1. Energy level diagram of $ScVO_4:Bi^{3+}$ (schematic). The trap depth associated with lattice defects is indicative.

The knowledge of the $Bi^{3+}(6s^2) \rightarrow V^{5+}(3d^0)$ MMCT energy (that corresponds to an electron transition from $^1S_0$ ground state of Bi^{3+} to the bottom of the host conduction band) allows locating the $^1S_0$ ground state at ≈ 2940 cm^{-1} above the top of the valence band. From this level, we locate the (V_O-perturbed) $^3P_1$ excited state in resonance with the CB edge. The dotted line in Fig. 1 figurates an excitation at 375 nm (26670 cm^{-1}). Considering ± 10 nm as the spectral bandwidth of the LED, this wavelength reaches the low energy sideband of the $Bi^{3+}(6s^2) \rightarrow V^{5+}(3d^0)$ MMCT and $6s^2$, $^1S_0 \rightarrow 6s^1p^1$, $^3P_1$ transitions of V_O-perturbed Bi^{3+} ions and, therefore, produces emission. The photoluminescence spectra of $ScVO_4:Bi^{3+}$ collected at 77 K for several monitored emission and excitation wavelengths are shown in Fig. 2.

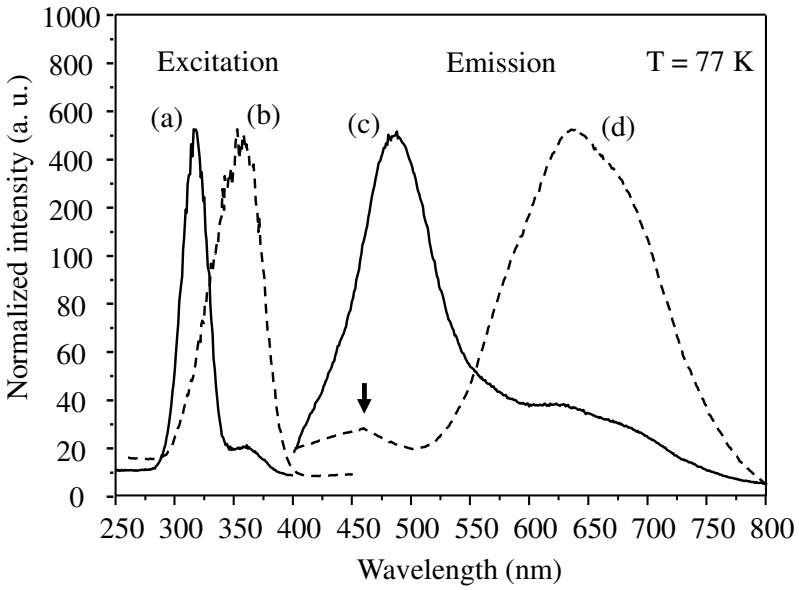

Fig. 2 – Steady state excitation spectra of $ScVO_4:Bi^{3+}$ with em = 500 nm (a) and em = 650 nm (b) and emission spectra with exc = 330 nm (c) and exc = 375 nm (d).

At this temperature, the energy transfer from the vanadate units to Bi^{3+} is less efficient compared to room temperature. This explains the presence of an emission band at 485 nm that appears upon inter-band excitation and is ascribed to $(VO_4)^{3-}$ groups. Moving the monitored wavelengths to the red reveals a second excitation band peaking at 360 nm (27780 cm^{-1}). This band matches the $Bi^{3+}(6s^2) \rightarrow V^{5+}(3d^0)$ MMCT and the $6s^2$, $^1S_0 \rightarrow 6s^1p^1$, $^3P_1$ transition of Vo-perturbed Bi^{3+}. This band is clearly individuated in the spectra because of the inefficient $(VO_4)^{3-} \rightarrow Bi^{3+}$ energy transfer at 77 K. Correspondingly, a broad red emission with complex

structure and a weak emission band in the blue spectral region (≈ 450 nm, see arrow in Fig. 2) are observed. Referring to the results reported in Ref. [3], we have collected the time-resolved emission spectra of $ScVO_4:Bi^{3+}$ at room temperature with delays ranging from 20 to 100 µs after the laser pulse (exc = 375 nm). Upon such conditions, the contribution from the $(VO_4)^{3-}$ groups vanishes and the obtained spectra account for the sole contribution of Bi^{3+} (Fig. 3).

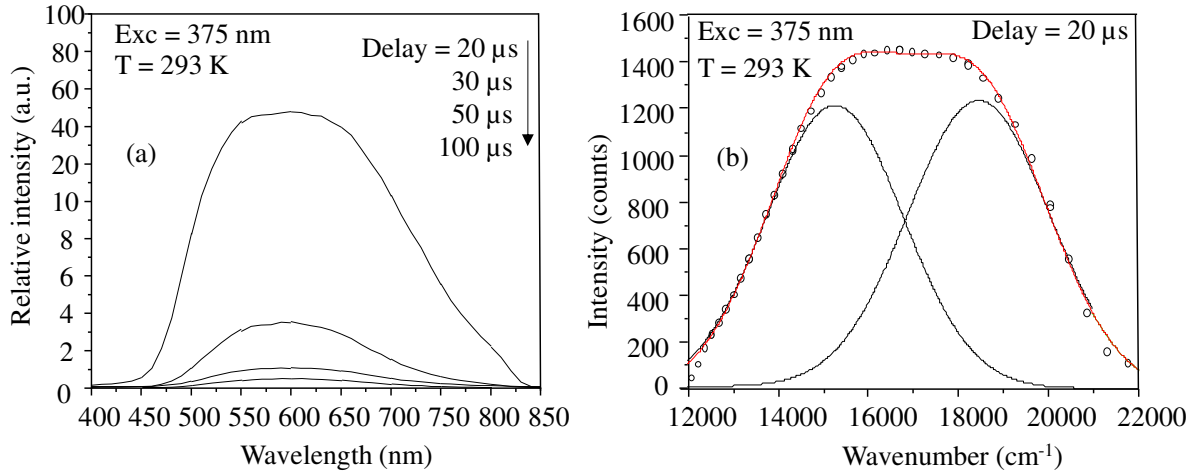

Fig. 3 – Time-resolved emission spectra of $ScVO_4:Bi^{3+}$ at room temperature for different delays after the laser pulse (a) and spectral decomposition of the time-resolved spectrum collected for a delay of 20 µs (b).

These spectra are broad (FWHM ≈ 0.80 eV) compared to the emission spectrum of the isostructural $YVO_4:Bi^{3+}$ (FWHM ≈ 0.54 eV [16]. The spectral decomposition of the spectrum collected 20 µs after the laser pulse gives two Gaussian bands with comparable spectral bandwidths (≈ 0.4 eV) peaking respectively at 542 nm (band I) and 644 nm (band II). The Stokes shifts associated with these emission bands amount 1.15 and 1.5 eV, respectively. We compare these data with those of several Bi^{3+}-doped vanadates in Table 1.

Table 1. Experimental position of lowest excitation and corresponding emission of Bi^{3+} in several vanadates. The Stokes shift is defined as the difference between the maxima. All energies expressed in cm^{-1}.

Compound	Excitation	Emission	Stokes shift	Assignment	Ref
$LiCa_3MgV_3O_{12}$	29355	17825	11530	Bi-V CT	22
$LaVO_4$	30860	18520	12340	Bi-V CT	10
$LuVO_4$	30080 30325	17095 17420	12985 12905	Bi-V CT	23 13

YVO_4	30485 29355 29355 30000 29600 28630	17660 17905 17580 17580 17180 17580	12825 11450 11775 12420 12420 11050	Bi-V CT	13 1 14 2 15 11
$GdVO_4$	30565 30565 29600 30485	17420 18065 18070 18870	13145 12500 11530 11615	Bi-V CT	13 2 24 10,12
$ScVO_4$	27745 27905 27780	15565 15725 15530 (band II) 18450 (band I) 22220 (77 K)	12180 12180 12250 9330 5560	A A, Bi-V CT Bi-V CT Bi-V CT A (Vo-perturbed)	2 7,5,20 this work this work this work

The attributes of band II are clearly those of a CT emission, as it was concluded earlier [20]. This means that the emission results from the radiative recombination of an exciton trapped at a formal Bi^{4+} site, with the electron delocalized among the nearest V^{5+} cations. For band I, the emission is green, as in other vanadates, and the Stokes shift exceeds 1 eV. This suggests that band I also has a CT nature. The observation of two Bi-related CT emissions is not much documented in the archival literature. Two exciton-like emissions, however, were identified in single crystalline films of $Lu_3Al_5O_{12}:Bi^{3+}$ and $Ga_3Ga_5O_{12}$ and ascribed to excitons localized respectively near a single Bi^{3+} ion or a Bi^{3+} dimer [25, 26]. In microcrystalline $Gd_3Ga_5O_{12}:Bi^{3+}$, emissions ascribed to excitons respectively trapped around single Bi^{3+} and around Bi^{3+} ions associated with lattice defects were found [27]. This is a possible option in the case of $ScVO_4:Bi^{3+}$, but we did not investigate this point further in the context of the present work. At last, we ascribe the weak blue emission observed 77 K with a Stokes shift below 1eV to a V_O-perturbed A state. As mentioned already, the V_O perturbation causes the energy downshift of the A excitation with concomitant shift of the A emission from the UV (where it is commonly observed in Bi^{3+}-doped compounds), to the blue spectral region.

With this in mind, we now show in Fig. 4 the variation of the intensity (*i. e.* integrated area) of the red emission of $ScVO_4:Bi^{3+}$ exposed to continuous LED irradiation at 375 ± 10 nm, at room temperature. Three different power densities were used for the LED.

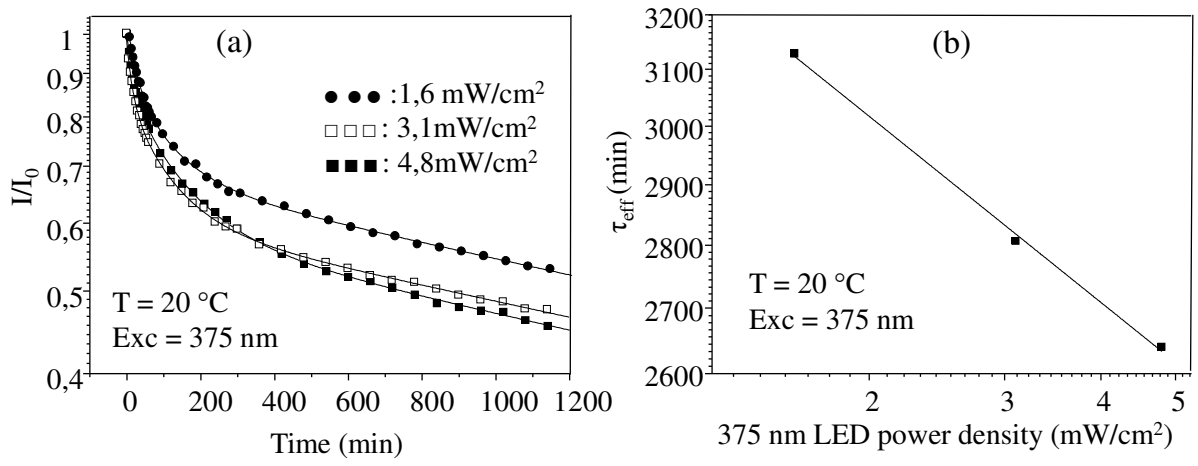

Fig. 4 – (a) Intensity of the red emission of $ScVO_4:Bi^{3+}$ *vs.* time at 20 °C. The solid lines figurate the fitting of the experimental data, see text. (b) Dependence of the effective degradation constant *vs.* the LED power (see text for details).

The observed kinetics look typical for phosphors in which the damages are due to photochemical processes affecting the luminescent activator in combination with the formation of a non-luminescent layer at the surface [28-30]. In the case of $K_2SiF_6:Mn^{2+}$, luminescence depreciation was observed at room temperature upon various irradiation power densities, just like in our experiment: the higher the irradiation power, the faster the decrease of the luminescence [30]. Following the methodology given in this work, we have reproduced the curves in Fig. 4 (a) by using $I(t) = \sum_{i=1}^{3} a_i \exp(-t/\tau_i)$ where *I(t)* is the luminescence intensity at time t, τ_i are the degradation constants and a_i are pre-exponential factors verifying $\sum_{i=1}^{3} a_i = 1$. The results of the fittings are compiled in Table 2 where τ_{eff} is the effective degradation constant defined as $\tau_{eff} = \sum_{i=1}^{3} a_i \tau_i$. This effective degradation constant depends on the irradiation power density *P* as $\tau_{eff} = \left(\frac{A}{P}\right)^n$. The corresponding Log-Log plot shown in Fig. 4(b) gives n = 0.155.

Table 2 – Parameters extracted from the fitting of Fig. 4(a)

LED power density (mW/cm2)	1.6	3.1	4.8
a_1	0.12	0.15	0.14
τ_1 (min)	26	17	20
a_2	0.20	0.25	0.28
τ_2 (min)	119	119	155
a_3	0.68	0.60	0.58
τ_3 (min)	4563	4625	4475
τ_{eff} (min)	3129	2807	2640

We show in Fig. 5 that the degradation of $ScVO_4:Bi^{3+}$ is strongly accelerated upon applying the following sequences: heating from 22 °C to 120 °C at a rate of 5 °C/min – holding at 120 °C for either 1 minute, 1 hour or 65 hours – then cooling to 22 °C according to the intrinsic inertness of the sample holder. In all the experiments, the excitation was 375 (± 10) nm and the luminescence intensity at time $t = 0$ and temperature $T_0 = 22$ °C (*i. e.* $I(T_0)$) was taken as reference.

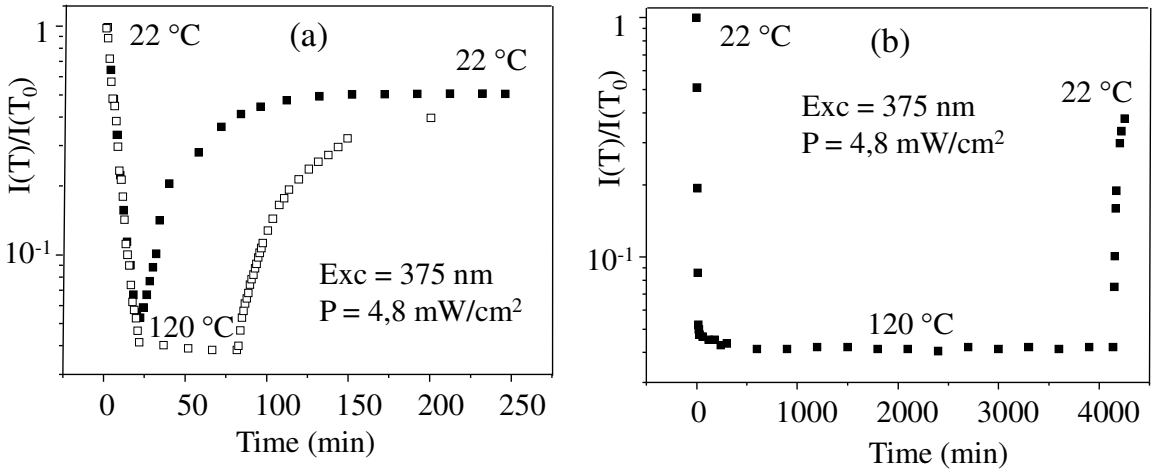

Fig. 5 – Intensity of the red emission of $ScVO_4:Bi^{3+}$ *vs.* time and temperature

We observe a rapid drop of the luminescence intensity upon warming to 120°C leading to the loss of 95 % of the initial intensity in 25 minutes. This fast depreciation includes two contributions: a reversible thermal quenching of the A and CT emitting states by thermal-assisted cross-over to the $^1S_0$ ground state of Bi^{3+}, combined with a physico-chemical degradation of the phosphor's surface. The irreversible character of this surface degradation is demonstrated by the partial restoration of the initial luminescence after coming back to room temperature. This phenomenon is almost independent on the holding time at 120 °C: the luminescence depreciation is ≈ 50 % for a holding time of 1 minute. (Fig. 5(a)) and ≈ 60 % for a holding time of 65 hours (Fig. 5(b)). We show in Fig. 6 the Arrhenius plots corresponding to Fig. 5(a), *i. e.* holding time of 1 or 60 minutes at 120 °C.

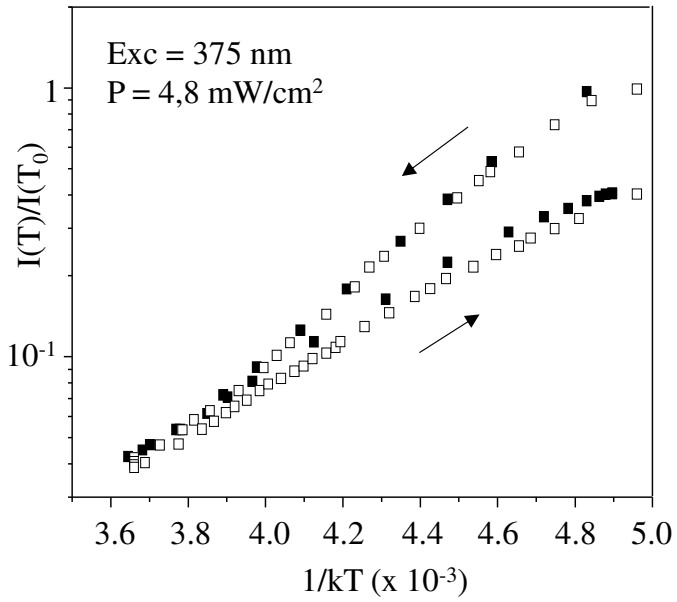

Fig. 6 – Arrhenius plots for the red emission of $ScVO_4:Bi^{3+}$ in correspondance with Fig. 5(a)

The curves are almost superimposable. Upon warming (decreasing arrow in Fig. 6), the variation (in Log scale) is linear up to 70°C and reproduced by the single energy barrier model $I(T)/I(T_0) = 1/[1 + A\exp(-\Delta E_q/kT)]$ where I(T) is the emission intensity a temperature T, $I(T_0)$ is the emission intensity at the reference temperature (here 295 K), A is the ratio between radiative and nonradiative rates and ΔE_q is the activation energy that is required for the emission quenching. Here, this energy amounts 1100 cm^{-1}, i. e. less than 1.5 times the maximum phonon energy of $ScVO_4$. It represents the energy gap separating between the minimum of the emitting state to its cross-over with the ground state. For T > 70°C (1/kT < 4.2 x10^{-3}), we observe slight deviation from linearity in the heating mode that reveals concomitant irreversible losses.

After aging, the surface color of $ScVO_4:Bi^{3+}$ systematically turns from bright yellow to brownish yellow. This is well illustrated by the remission (Kubelka-Munk) functions F(R) calculated from the reflectivity spectra of a virgin and aged sample (Fig. 7). The difference $F(R)_{aged} - F(R)_{virgin}$ is displayed in inset. This experiment reveals a lower number of centers absorbing at ≈ 380 nm (Bi^{3+}-related) and ≈ 450 nm (lattice defects like $[V^{4+}]_A$ centers [6]) after aging.

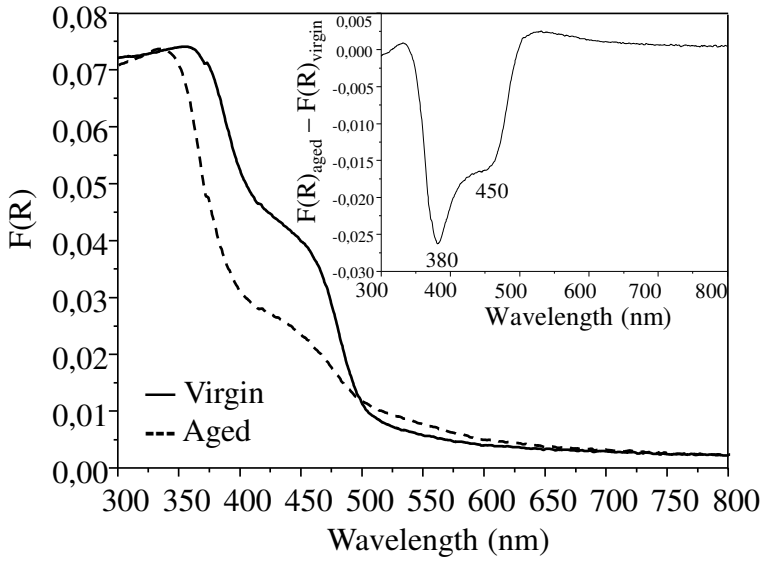

Fig. 7 - Remission spectra of $ScVO_4:Bi^{3+}$ at 20 °C (virgin: solid line, aged: dotted line). The inset shows the wavelength dependence of the difference $F(R)_{aged} - F(R)_{virgin}$

These results are consistent with a persistent photo-stimulated oxidization of surface Bi^{3+} and subsequent trapping of charge carriers by lattice defects responsible for the yellow color of the virgin pigment (*i. e.* like the $[V^{4+}]_A$ centers [6]): the formation of surface Bi^{4+} decreases the Bi^{3+} amount and reduces the luminescence, while the trapping of charge carriers by $[V^{4+}]_A$ centers bleaches the pigment surface. New absorbing centers result from this aging process; they give a brown coloration of the pigment surface that contributes to further lower the luminescence by self-absorption. To our knowledge, this deleterious process is specific to $ScVO_4:Bi^{3+}$. We ascribe it to the presence of oxygen vacancies and V^{4+} ions adjacent to Bi^{3+} that promote the dissociation of the Bi-V trapped exciton by electron trapping, with concomitant hole trapping at the Bi^{4+} site (Fig. 1). EPR and photostimulated EPR spectra were collected to confirm this scenario, but these spectra are very complex and their analysis still in progress. These results, combined with thermoluminescence measurements, will be compiled in a forthcoming report.

4. Conclusion

Significant luminescence depreciation is evidenced at room temperature in $ScVO_4:Bi^{3+}$ upon continuous LED irradiation at 375 nm at a power density of 4.8 mW/cm^2. In these conditions, the depreciation amounts 50% of the initial emission intensity in 13 hours. Further, the compound losses 95 % of its initial luminescence intensity in 25 minutes upon warming to 120 °C. These deleterious phenomena are specific of $ScVO_4:Bi^{3+}$ and are ascribed to the

photo-stimulated oxidization of surface Bi^{3+} favored by the presence of lattice defects in the immediate neighborhood of this ion. Additional experiments based on EPR and thermoluminescence are in progress to confirm this scenario.

Acknowledgments

We are grateful to Professor Mingying Peng [1978 - 07 – 2020 - 11] from the China-Germany Research Center for Photonic Materials and Devices, The State Key Laboratory of Luminescent Materials and Devices and the Institute of Optical Communication Materials, School of Materials Sciences and Engineering, South China University of Technology, Guangzhou 510641, China for providing the $ScVO_4$:1%Bi^{3+} sample. F. Kang acknowledges financial support from European Union's Horizon 2020 research and innovation program under the Marie Sklodowska-Curie grant agreement no. 713683 (COFUNDfellowsDTU)

References

[1] G. Blasse, A. Bril, Investigations on Bi^{3+}-activated phosphors, J. Chem. Phys. 48 (1968) 217-222

[2] G. Boulon, Processus de photoluminescence dans les oxydes et les orthovanadates de terres rares polycristallins, activés par l'ion Bi^{3+}, J. de Physique, 32 *(*1971) 333-347.

[3] F. W. Kang, X. B, Yang, M. Y. Peng, L. Wondraczek, Z. J. Ma, Q. Y. Zhang, J. R. Qiu, Red photoluminescence from Bi^{3+} and the influence of the oxygen perturbation in $ScVO_4$: a combined experimental and theoretical study, J. Phys. Chem. C, 118 (2014) 7515-7522.

[4] F. W. Kang, Y. Zhang, L. Wondraczek, J. Q. Zhu, X. B. Yang, M. Y. Peng, Processing dependence and the nature of the blue-shift of Bi^{3+}-related photoemission in $ScVO_4$ at elevated temperatures, J. Mater. Chem. C, 2 (2014) 9850-9857.

[5] H. S. Zhang, F. W. Kang, Y. J. Zhao, M. Y. Peng, D. Y. Lei, X. B. Yang, The role of oxygen defects in a bismuth doped $ScVO_4$ matrix: tuning luminescence by hydrogen treatment, J. Mater. Chem C, 3 (2017) 314-321.

[6] N. Y. Garces, K. T. Stevens, G. K. Foundos, L. E. Halliburton, Electron paramagnetic resonance and optical absorption study of V^{4+} centres in YVO_4 crystals, J. Phys.: Condens. Matter., 16 (2004) 7095-7106.

[7] F. W. Kang, G. H. Sun, P. Boutinaud, F. Gao, Z. H. Wang, J. Lu, Y. Y. Li, S. S. Xiao, Tuning the Bi^{3+}-photoemission color over the entire visible region by manipulating secondary

cations modulation in the $ScV_xP_{1-x}O_4:Bi^{3+}$ ($0 \leq x \leq 1$) solid solution, J. Mater. Chem. C, 7 (2019) 9865-9877.

[8] P. Boutinaud, Revisiting the spectroscopy of the Bi^{3+} ion in oxide compounds, Inorg. Chem. 52 (2013) 6028-6038.

[9] R. Moncorgé, G. Boulon, Investigations of the absorption and emission properties along with energy transfer in pure and Bi^{3+} doped YVO_4, J. Lumin. 18/19 (1979) 376-380.

[10] M. Amer, P. Boutinaud, On the character of the optical transitions in closed-shell transition metal oxides doped with Bi^{3+}, Phys. Chem. Chem. Phys., 19 (2017) 2591-2596.

[11] E. Cavalli, F. Angiuli, F. Mezzadri, M. Trevisani, M. Bettinelli, P. Boutinaud, M. G. Brik, Tunable luminescence of Bi^{3+}-doped $YP_xV_{1-x}O_4$ ($0 \leq x \leq 1$), J Phys: Condens Matter. 26 (2014) 385503.

[12] P. Boutinaud, E. Cavalli, Predicting metal-to-metal charge transfer in closed shell transition metal oxides doped with Bi^{3+}, Chem. Phys. Lett. 503 (2011) 239-243.

[13] A. Krasnikov, V. Tsiumra, L. Vasylechko, S. Zazubovich, Ya. Zhydachevskyy, Photoluminescence origin in Bi^{3+}-doped YVO_4, $LuVO_4$ and $GdVO_4$, J. Lumin. 212 (2019) 52-60.

[14] R. Moncorge, G. Boulon, Investigation of the absorption and emission properties along with energy transfer in pure and Bi^{3+}-doped YVO_4, J. Lumin. 18/19 (1979) 376-380.

[15] S. Mahlik, M. Amer, P. Boutinaud, Energy Level Structure of Bi^{3+} in Zircon and Scheelite Polymorphs of YVO_4, J. Phys. Chem C. 120 (2016) 8261-8265.

[16] A. Krasnikov, E. Mihokova, M. Nikl, S. Zazubovich, Y. Zhydachevskyy, Luminescence spectroscopy and origin of luminescence centers in Bi-doped materials, Crystals 10 (2020) 208.

[17] A. M. Srivasrava, Luminescence of Bi^{3+} in the orthorhombic perovskites $CaB^{4+}O_3$ (B^{4+} = Zr, Sn): crossover from localized to D-state emission, Opt. Mater. 58 (2016) 89-92.

[18] A. M. Srivastava, W. W. Beers, On the impurity trapped exciton luminescence in $LaZr_2O_7:Bi^{3+}$, J. Lumin. 81 (1999) 293-300.

[19] A. M. Srivasrava, Luminescence of Bi^{3+} in the orthorhombic perovskites $SrB^{4+}O_3$ (B^{4+} = Zr, Sn), Opt. Mater. 58 (2017) 313-315.

[20] P. Boutinaud, M. G. Brik, The optical properties of Bi^{3+} and Sb^{3+} in $YNbTiO_6$ analysed by means of DOS and semi-empirical calculations, J. Mater. Chem. C 8 (2020) 2086-2093.

[21] Anthony Barros, PhD Thesis, Clermont-Ferrand, June 2016

[22] P. Dang, S. Liang, G. Li, Y. Wei, Z. Cheng, H. Lian, M. Shang, A. A. Al Kheraif, J. Lin, Full color luminescence tuning in Bi^{3+}/Eu^{3+}-doped $LiCa_3MgV_3O_{12}$ garnet phosphors based on local lattice distortion and multiple energy transfers, Inorg. Chem. 57 (2018) 9251-9259.

[23] F. W. Kang, M. Y. Peng, Q. Y. Zhang, J. R. Qiu, Abnormal anti-quenching and controllable multi-transitions of Bi^{3+} luminescence by temperature in a yellow-emitting $LuVO_4:Bi^{3+}$ phosphor for UV-converted white LEDs, Chem. - Eur. J., 20 (2014)11522-11530.

[24] B. N. Mahalley, S. J. Dhoble, R. B. Pode, G. Alexander, Photoluminescence in $GdVO_4$:Bi^{3+},Eu^{3+} red phosphor, Appl. Phys. A. 70 (2000) 39-45.

[25] V. Babin, V. Gorbenko, A. Krasnikov, A. Makhov, M. Nikl, K. Polak, S. Zazubovich, Yu Zorenko, Peculiarities of excited state structure and photoluminescence in Bi^{3+}-doped $Lu_3Al_5O_{12}$ single crystalline films, J. Phys.: Condens. Matter 21 (2009) 415502.

[26] A. Krasnikov, A. Luchechko, E. Mihokova, M. Nikl, I. I. Syvorotka, S. Zazubovich, Ya. Zhydachevskii, Origin of Bi^{3+}-related luminescence in $Gd_3Ga_5O_{12}:Bi^{3+}$ epitaxial films, J. Lumin. 190 (2017) 81-88

[27] V. Tsiumra, A. Krasnikov, S. Zazubovich, Ya. Zhydachevskii, L. Vasylechko, M. Baran, L. Wachnicki, L. Lipinska, M. Nikl, A. Suchocki , Crystal structure and luminescence studies of microcrystalline GGG:Bi^{3+} and GGG:Bi^{3+}, Eu^{3+} as a UV-to-VIS converting phosphor for white LEDs, J. Lumin. 213 (2019) 278-289.

[28] U. Vater, G. Küntzler, W. Tews, Quenching problems in inorganic luminescent materials, J. Fluorescence 4 (1994) 79.

[29] W. Tews, U. Vater, G. Küntzler, U. Sasum, A. Kloss, The stability of inorganic oxygen dominated phosphors under the influence of UV radiation or a Hg-Ar discharge, Phys. Stat. Sol. (a) 130 (1992) K131.

[30] T. Oyama, S. Adachi, Unique light-induced degradation in yellow-emitting $K_2SiF_6:Mn^{2+}$ phosphor, J. Appl. Phys. 116 (2014) 133515.